Hindawi
Adsorption Science & Technology
Volume 2023, Article ID 4596086, 12 pages
https://doi.org/10.1155/2023/4596086

Research Article

Contribution Evaluation of Physical Hole Structure, Hydrogen Bond, and Electrostatic Attraction on Dye Adsorption through Individual Experiments

Wengang Wang,[1,2] Lei Wang,[1,2] Ming Zhang,[1,2] Bo Yu,[1,2] Xiaoning Li,[1,2] and Han Yan[1,2]

[1]*China Tiegong Investment & Construction Group Co., Ltd., Beijing 100000, China*
[2]*China Railway Water Group Co., Ltd., Xi'an 710000, China*

Correspondence should be addressed to Ming Zhang; mingzhang1993@sina.com

Received 8 October 2022; Revised 20 December 2022; Accepted 16 January 2023; Published 27 January 2023

Academic Editor: Anjani Ravi Kiran Gollakota

Disagreements over various unanswered questions about contribution of the adsorption process and functional groups on dye adsorption still exist. The main aim of this research was to evaluate the contributions of physical hole structure, hydrogen bond, and electrostatic attraction on dye adsorption. Three ideal representatives, namely, a sponge with porous structure, P(AM) containing -$CONH_2$ groups, and P(AANa/AM) containing -COONa groups, were chosen to evaluate the above contributions. The methylene blue (MB) removal rates of these three products were compared through individual experiments. The results revealed that physical hole structure did not play a role in decreasing dye concentration. Hydrogen bond existed in dye adsorption but did not remarkably reduce dye concentration. The excellent removal results of P(AANa/AM) demonstrated that electrostatic attraction was critical in enriching dye contaminants from the solution into solid adsorbent. The results could provide insights into the dye adsorption mechanisms for further research.

1. Introduction

Much attention has been paid to the exponential growth of dye pollution. These pollutants are released from contemporary industries and chemical laboratories [1–3]. Coloring materials have high chromaticity, which sets them apart from other types of traditional organic pollutants, such as lipids or carbohydrates. If dyes are released straight into the natural rivers without any treatment, the water will be contaminated and turn into a red, blue, yellow, or other colored environment. However, microbial degradation has a poorer removal effectiveness than chemical separation techniques for a high-concentration dye wastewater [4–6]. Moreover, a bioreactor can maintain a high residue level of dye pollutants for an extended period of time. By contrast, adsorption treatment has a potential efficacy in removing dye contaminants and could be regarded as a large-scale and rapid method to transfer pollutants from a solution into solid adsorbents [7, 8].

Various adsorption materials, including modified agricultural wastes, synthesized high-molecular polymers, and advanced materials, have been reported for dye removal [9–11]. On the one hand, the adsorption capacities of adsorbents have been developed through innovating traditional preparation methods. On the other hand, extensively modified adsorbents, such as hydrogel loaded with magnetic materials and small-molecular substances packaged by large porous materials, have been prepared to enhance their recycling convenience [12, 13]. Previous studies have described adsorption functions, including physical hole structure, electrostatic attraction, or hydrogen bonds with N and O atoms to H atom, to explain the adsorption mechanisms. The porous properties of adsorbents have been obtained by scanning electron microscopy (SEM) observation or Brunauer-Emmett-Teller (BET) surface area analysis. Typical porous materials, such as active carbon and zeolite, exhibit excellent dye adsorption capacity [14–16]. However, although dye concentration can be decreased by activated carbon or

zeolite, the conclusion that physical hole structure in activated carbon or zeolite plays a crucial role in decreasing dye concentration may still not be drawn. The reason for this statement is that the compositions of the reported adsorbents are complex. In addition, the existence of porous structure was emphasized in the mass transfer from aqueous solution into solid adsorbents. However, the contribution of each part of adsorbents on dye adsorption should still be evaluated from contrast experiments. Functional groups, like hydroxide radical (-OH), amidogen ($-NH_2$), and carboxyl ($-COO^-$), have adsorption forces that fix dye pollutants. Wang et al. reported that the outstanding adsorption capacity of acrylic acid-functionalized graphene for cationic dyes was attributed to electrostatic interaction, π-π conjugation, and hydrogen bonding [17]. Silva et al. revealed that -OH and $-NH_2$ groups in chitosan exerted main roles in the removal of cationic basic blue 7 dye [18]. Chen et al. accounted that hydrogen bond could be an adsorption force between $-CONH_2$ and methylene blue (MB) dye [19]. Xu et al. gave an account that the hydroxyalkylaminoalkylamide groups on the six-membered ring of β-cyclodextrin enhanced the porous network capture ability for congo red dye [20]. Fan et al. interpreted that amino $-NH_2$ and azo -N=N- groups in cationic dyes could interact with carboxylic $-COO^-$ groups in hydrogels [21]. Seera et al. manifested that $-NH_2$ in gelatin can connect with MB through forming hydrogen bond with $-NH_2$ and N atoms in MB molecules [22]. Hafdi et al. explained that the adsorption mechanism of nickel oxide-doped natural phosphate (NP/NiO) was the formation of hydrogen bond between hydroxyl groups in nanoparticles and N atoms in dye [23]. Jiang et al. demonstrated that the high adsorption capacity of modified β-cyclodextrin could be partly ascribed to the complexation and network capture by its special cavity structure [24]. In conclusion, the adsorption action of hydrogen bond in mixed systems containing various functional groups has been described. Hydrogen bond existed in a form of covalent bond between H atom and electronegative atoms. And the electronegative atoms included N and O atoms [25, 26]. However, the contribution of hydrogen bond on dye adsorption has not yet been quantified. Whether hydrogen bond would greatly decrease dye concentration remains in doubt. Up to now, the essence of adsorbents in adsorbing pollutants has not been explained clearly and definitely. Therefore, a series of single-factor evaluation experiments should be designed and conducted to determine the crucial adsorption force on dye adsorption.

The -COONa functional group has been applied in adsorbents to adsorb dye pollutants. Moreover, the -COONa groups are widely used in super absorbent resin, which can absorb water and retain water molecules in network structures [27–29]. Hence, the same property of -COONa groups that absorbs water molecules might also be applicable for dye adsorbents. Early studies have focused on the adsorption capacities of adsorbents or the removal rates for dye pollutants. Batch experiments, such as the kinetic model fitting for time-dependent curves and the calculation of parameters in thermodynamic models, have been conducted to clarify the basic characteristics of dye adsorbents [30]. The focus of these models is to explain the trends of the adsorption capacity for adsorbents and the pollutant removal rates. However, the swelling characteristics of adsorbents containing -COONa group in dye solution have not been investigated. Studies that observed the dynamic changes of adsorbent during the entire dye adsorption process are limited. The contribution of each part of an adsorbent, including the physical hole structure and various functional groups on dye adsorption, has not been evaluated individually. The dynamic changes might include the water absorption or swelling behavior of adsorbents during the dye adsorption process.

In this work, the contributions of physical hole structure, hydrogen bond, and electrostatic attraction on dye adsorption were evaluated through individual experiments. Three ideal representatives, namely, a sponge with physical hole structure, P(AM) with $-CONH_2$ groups, and P(AANa/AM) with -COONa groups, were chosen to evaluate the above contributions. Especially, P(AM) and P(AANa/AM) were prepared by graft copolymerization. These two products were used to evaluate the dye enrichment properties of hydrogen bond by $-CONH_2$ and electrostatic attraction by -COONa. Meaningful evaluation experiments were conducted for these three single component materials. The MB removal rates of the three representatives were compared to assess the effect on decreasing dye concentration. The morphologies of the three representatives in MB solution were also focused synchronously to provide the favorable evidence. The adsorption performance of the electrostatic attraction between -COONa in the P(AANa/AM) product and MB was investigated thoroughly under bottle shaking and column adsorption experiments. This research would be bound to have an important impact on dye adsorption mechanisms.

2. Materials and Methods

2.1. Materials. Acrylic acid (AA), acrylamide (AM), ammonium persulfate (APS), N,N-methylene bisacrylamide (MBA), sodium hydroxide (NaOH), methylene blue (MB), hydrochloride acid (HCl), and sodium chloride (NaCl) were purchased from Kelong Chemical Reagent Plant (Chengdu, China). The above chemical reagents were analytical grade. The sponge was purchased from Zhengzhou Fengtai Nanomaterials Co., Ltd. (Zhengzhou, China).

2.2. Product Preparation. Three products, including P(AM), P(AANa), and P(AANa/AM), were synthesized by graft copolymerization in solution. The main components of P(AANa/AM) were composed of sodium carboxylate (-COONa) and acylamino ($-CONH_2$) in polymer chains. The adsorption capacity of -COONa was assessed using P(AM) with $-CONH_2$ groups. P(AANa) and P(AANa/AM) gels were used as the intermediate polymerization products to conduct the mechanical experiment for observing the role of AM in the P(AANa/AM) product. Firstly, 5 mL of AA with 100% neutralization degree by 10 wt.% NaOH, 2 g of AM, and 0.30 g of MBA were mixed in a 100 mL breaker under constant magnetic stirring at 70°C. Then, the APS

solution (0.20 g of APS to 5 mL of distilled water) was added. When the mixture turned into a gel, the magnetic stirrer was turned off, and the reaction was continued for 3 h. In addition, under the same APS and MBA doses, P(AM) was prepared with 7.0 g of AM and no addition of AA, and P(AANa) was prepared with AA and no addition of AM. Finally, the gel was cut and dried at 70°C. The products had a particle size in the range of 0.45 mm to 1 mm.

2.3. MB Adsorption Experiments. The main MB adsorption force of the functional groups in P(AANa/AM) was investigated. The polymer chains of the P(AANa/AM) product included -$CONH_2$ and -COONa, whereas those of the P(AM) contained -$CONH_2$ groups. Methylene blue solutions with various concentrations were prepared using distilled water. Then, 0.05 g of the dried particles was added into 50 mL of the solution at 25°C. The determination experiments of water absorbency were conducted from three individual measurements. After reaching the equilibrium state, the concentration of MB in the residual solution was detected using a UV-vis spectrometer (UV-1800, Shimadzu, Japan). The adsorption capacity (Q_a) and removal rate (η) to MB were calculated:

$$Q_a = \frac{(C_0 - C_e) \times V}{m}, \quad (1)$$

$$\eta = \frac{C_0 - C_e}{C_0} \times 100\%, \quad (2)$$

where Q_a means the adsorption capacity of product (mg/g), η means the removal rate to MB (%), C_0 and C_e mean the initial equilibrium concentration (mg/L), V is the volume of MB solution (L), and m is the weight of the dried products (g).

Based on the shaking flask adsorption experiments, dynamic column adsorption experiments were also established. With the effective height of 10 cm, 0.15 g of the dried P(AANa/AM) particles was loaded into the glass column. The upward flow was 5 mL/min by using a peristaltic pump to inject 20 mg/L MB solution for 30 min. The MB concentration in effluent was detected with an interval of 2 min.

2.4. Measurement of Water Absorbency. The swelling properties of P(AANa) and P(AANa/AM) were determined by the gravimetric method. In particular, a sponge block was applied to determine the water holding property of physical hole structure. The dried samples (0.1 g) were immersed in 100 mL distilled water or 20 mg/L MB solution. After the samples were saturated, filtered, and weighted, water absorbency was calculated:

$$Q_b = \frac{m_2 - m_1}{m_1}, \quad (3)$$

where Q_b is the water absorbency of product (g/g), m_1 is the weight of the dried samples (g), and m_2 is the weight of samples for absorbing water (g).

2.5. Characterization. The compressive strengths of the polymerized gels were determined using the universal material testing machine (Instron 5967, England) at the compression rate of 10 mm/min. The samples were in the shape of a cylinder (diameter of 2 cm and height of 3 cm). The end of compression ratio was 70%. The macroappearance and the microtopography of the products after immersion in MB solution were observed using the reflected light microscope (ZEISS Stemi SV 11, Shanghai, China) and scanning electron microscopy (SEM, Apreo S, USA). The samples were filtered and photographed after immersion in distilled water or MB solution. For SEM observation, the swollen particles were dried by vacuum freeze dryer. The dried specimens were placed carefully on conducting glue coated with gold vapor to confer conductivity. A Nikon camera was used to photograph the morphology in the column experiment.

3. Results and Discussion

3.1. Role of AM in P(AANa/AM). The P(AANa/AM) product consisted of two hydrophilic groups, namely, -$CONH_2$ and -COONa, in the polymer chains. The final removal state to dye pollutants is the transferring and enriching process from the solution into adsorbents. Figure 1(a) shows the MB removal rates of P(AM) and P(AANa/AM) in 20 mg/L MB solution under different adding doses. Obviously, the MB removal rate by P(AM) increased linearly when the weight of P(AM) increased from 0.01 g to 0.05 g. More remarkable, when the weight of P(AM) increased further, the MB removal rates were kept a relatively stable state and all were lower than 80%. However, for P(AANa/AM), the average MB removal rates under different adding doses were 97.06% ± 0.60%. In particular, P(AM) was synthesized by AM under graft copolymerization, in which functional group was -$CONH_2$. P(AANa/AM) was synthesized by AA and AM under neutral condition and graft copolymerization, in which the functional groups were -$CONH_2$ and -COONa. Comparisons of the structure and composition differences between P(AM) and P(AANa/AM) showed that -COONa in the polymer chains was the remarkable characteristic of P(AANa/AM) for MB removal. More deeply, P(AM) containing -$CONH_2$ groups exhibited the dye combination property with the dye but did not achieve a great effect in enriching dye molecules. On the contrary, -COONa in P(AANa/AM) belongs to ionic functional groups, which showed excellent performance in combining with MB pollutant [31]. The comparison results showed that -$CONH_2$ in AM was not crucial in MB adsorption. However, AM was one of the indispensable raw materials to synthesize P(AANa/AM). Thus, necessary experiment should be conducted to investigate the actual contribution of AM in P(AANa/AM).

Figure 1(b) shows the compressive strength results of the P(AANa) and P(AANa/AM) gels, respectively. Under the same cracking moment, the compressive strength of the polymerized gel increased from 49.80 kPa to 278.66 kPa. The vital promotive role of AM was not to increase the capacity of the adsorbent to adsorb MB solution, but to strengthen the mechanical property of the polymerized gel.

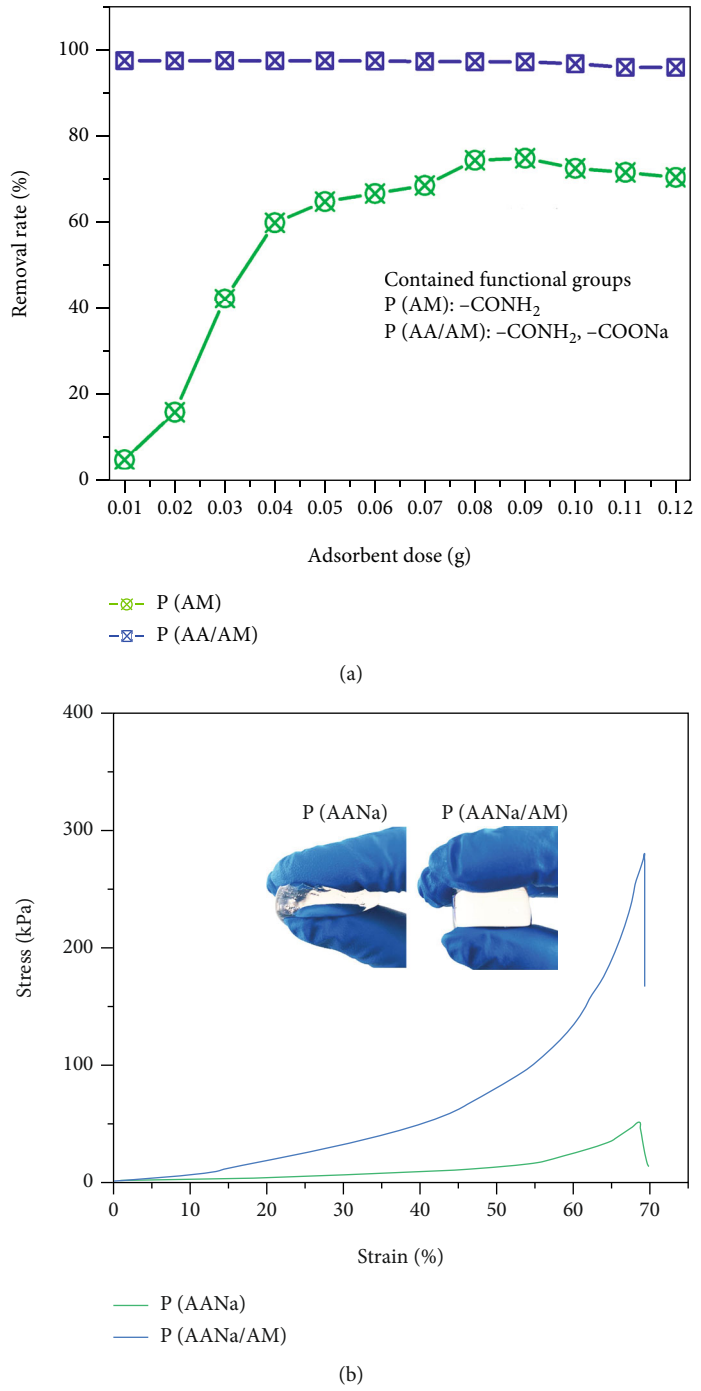

Figure 1: (a) Effect of adsorbent dose to MB removal rate. (b) Compressive strain-stress curves of P(AANa) and P(AANa/AM) gels.

At the late product preparation process, an essential step was to cut the polymerized gel into small cubes. Thus, the gel with strong mechanical strength contributed to this process.

3.2. Dye Adsorption and Swelling Property. The removal process of dye pollutants involved the migration and binding process for dye molecules. Two indexes, namely, MB removal rate and water absorbency, were observed to evaluate the interaction between P(AANa/AM) and dye pollutants. Table 1 and Figure 2 show the removal rate and water absorbency results for sponge, P(AM), and P(AANa/AM), respectively. Porous sponge had no MB adsorption capacity and exhibited the water absorption capacity of 135.29 g/g in distilled water and 135.50 g/g in 20 mg/L MB solution. Porous sponge could absorb water when immersing in MB solution. The color of the sponge block turned into blue, but the concentration of MB solution did not decrease. MB molecules were moved out from the sponge by squeezing. In comparison, the porous structure in adsorbents was favorable for the migration of dye pollutants from

Table 1: Comparison of the MB removal rate and water absorbency for sponge, P(AM), and P(AANa/AM).

	Removal rate to MB (%)	Water absorbency (g/g)	
		Distilled water	MB solution
Sponge	0	135.29	135.50
P(AM)	64.88	7.51	7.48
P(AANa/AM)	97.44	53.80	53.74

the solution into the adsorbent's inner areas. However, whether physical hole structure could decrease dye concentration had not been concerned in literatures. The porous sponge did not cause a remarkable decrease in MB concentration. These individual experiments confirmed that the physical hole structure in adsorbents did not contribute to dye adsorption.

Across the same dose and dye concentration, the dye removal rate of 97.44% by P(AANa/AM) was quite higher than that of 64.88% by P(AM). P(AM) and P(AANa/AM) products produced under the graft copolymerization reaction and contained the polymeric network structure. The partial decrease in MB concentration by P(AM) was ascribed to the hydrogen bond between P(AM) and MB molecules, rather than the polymer chains. For P(AM), several -$CONH_2$ groups were linked at the main polymer chains. The hydrogen bond between -$CONH_2$ and MB molecules caused the decrease in MB concentration. For P(AANa/AM), the electrostatic attraction between -COONa and MB molecules achieved an excellent dye removal effect. This result indicated that the electrostatic attraction had a crucial impact on removing dye pollutants from the solution into the solid adsorbents. Specifically, -COONa groups were classified as an anionic group, which could combine with cationic MB molecules [32, 33]. Based on this form, MB molecules could be enriched and fixed in the inner area of P(AANa/AM). Overall, the binding force that remarkably decreased MB concentration was the electrostatic attraction, not hole structure and hydrogen bond.

The water-absorbing behavior of P(AANa/AM) in dye solution was also observed. The sponge, P(AM), and P(AANa/AM) all absorbed water when immersed in distilled water or MB solution. The swelling phenomena for P(AM) and P(AANa/AM) were accompanied with dye adsorption behavior. Particle size was increased obviously after adding the dried products into distilled water or MB solution. Thus, previous insights about dye adsorption process were partially limited. The swelling behaviors of dried P(AM) and P(AANa/AM) particles were ascribed to their obtained functional groups and polymer network structure. In fact, -$CONH_2$ and -COONa groups are hydrophilic groups. With the cooperation of polymer network structure, these groups presented the water combination property. Furthermore, the mutual repulsive force for -COONa groups aggravated the expansion of the polymer chains. This property was also confirmed from the water absorbency difference between P(AM) and P(AANa/AM). The hydrophilic groups in the polymer chains, including -$CONH_2$ and -COONa, could combine water and MB molecules through hydrogen bond and electrostatic attraction. A new insight was put forward that the morphological changes, especially the swelling behavior, should be listed as an index to study the dye pollutant removal mechanisms.

3.3. SEM Observation. Figure 3 shows the SEM images of P(AANa/AM) and sponge. The dense and solid structure of the P(AANa/AM) surface after dehydration and drying treatments during preparation is displayed in Figure 3(a). After soaking the dried particles into 20 mg/L MB solution, the particle size increased as shown in Figure 3(b). The interwoven polymer chains of the swollen particles were a testament to the ease and practicability of graft polymerization. Hydrophilic functional groups, such as -$CONH_2$ and -COONa, allowed the stretching of the polymer chains. Water molecules were immobilized in the polymer network structure. As a result, the water absorption process was coupled with the dynamic dye adsorption process. Finally, P(AANa/AM) particles were no longer the original dried particles but became an extended gel once the dye adsorption equilibrium condition was reached. Figure 3(c) shows the SEM image of the physical hole structure of sponge. The visible porous structure in the sponge revealed that sponge could be an ideal representative to evaluate the contribution of physical hole structure on dye adsorption.

Figure 4 provides the morphological variations of P(AANa/AM) during the product preparation and MB adsorption processes. The formation of free radicals at AA and AM was assisted by the initiator APS. All single monomers took part in chain growth and formed the long chain polymer. In addition, the dissolved AA and AM raw materials were transformed into a translucent huge gel by the crosslinking agent MBA. The gel had a water content of roughly 86%. The gel was then sliced with scissors into tiny cubes. After the cubes were dried, milled, and sifted, the P(AANa/AM) adsorbents were obtained as dried, shrank particles. Two hydrophilic functional groups, namely, -$CONH_2$ and -COONa, were located at the polymer-branched chains. After the dried P(AANa/AM) particles were soaked into MB solution, the dye adsorption phenomenon could be clearly observed, which was accompanied by a remarkable decrease in MB concentration. Furthermore, the final state of P(AANa/AM) was the expanded hydrogel, where large amounts of water molecules were stored in the inner of adsorbent. This unique characteristic of the adsorbent brought the ease in the diffusion and migration for MB molecules. Moreover, the stretched polymer chains have a high efficiency for the combination reaction between -COONa groups and MB molecules [32–34].

3.4. Confirmation of Adsorption Force. Figure 5 shows the MB removal rate results of P(AM) and P(AANa/AM) under various low concentrations of MB. It can be seen that the removal rates of MB by P(AANa/AM) were all considerably higher than those by P(AM). The MB removal rate by P(AM) was 15.31% when the initial MB concentration was 1 mg/L. Further increasing the initial MB concentration,

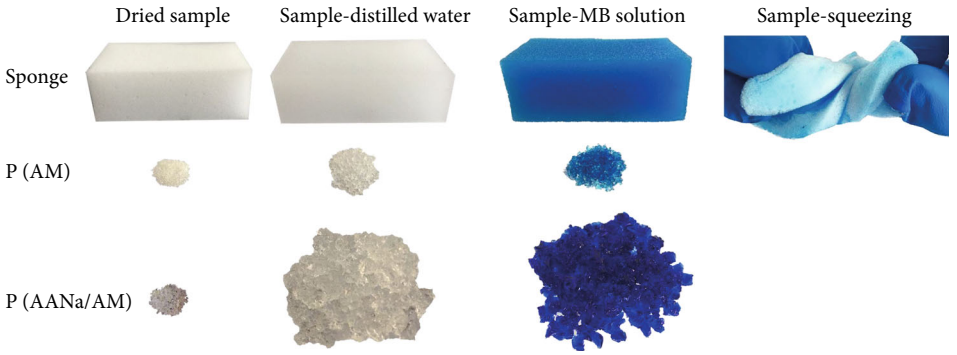

Figure 2: Macromorphologies of sponge, P(AM), and P(AANa/AM) immersed in distilled water and 20 mg/L MB solution.

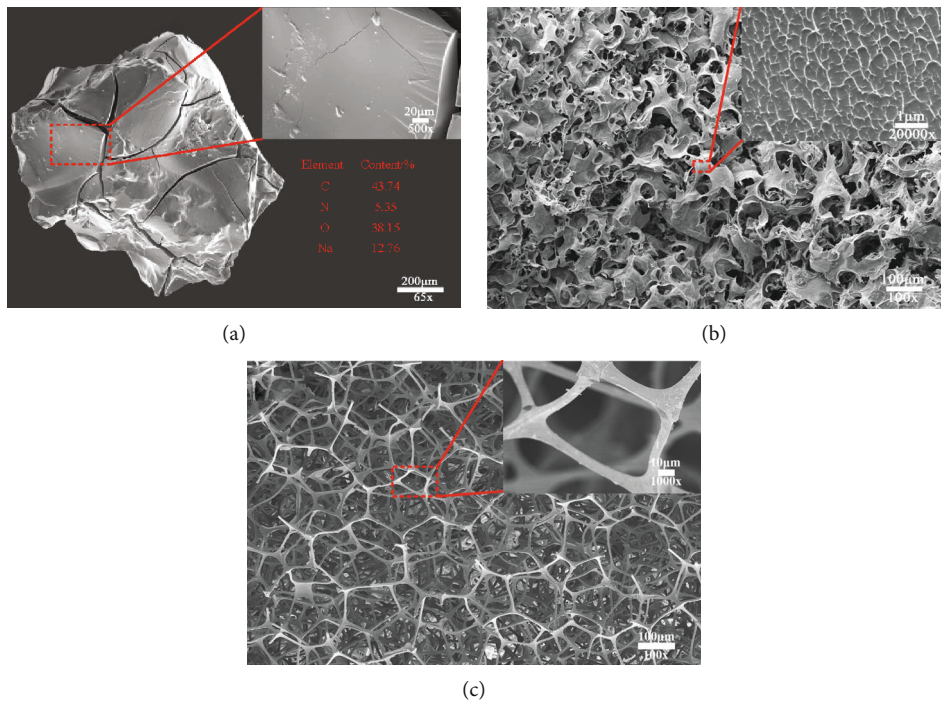

Figure 3: SEM images of (a) dried P(AANa/AM) particles, (b) P(AANa/AM) immersed in MB solution, and (c) the sponge.

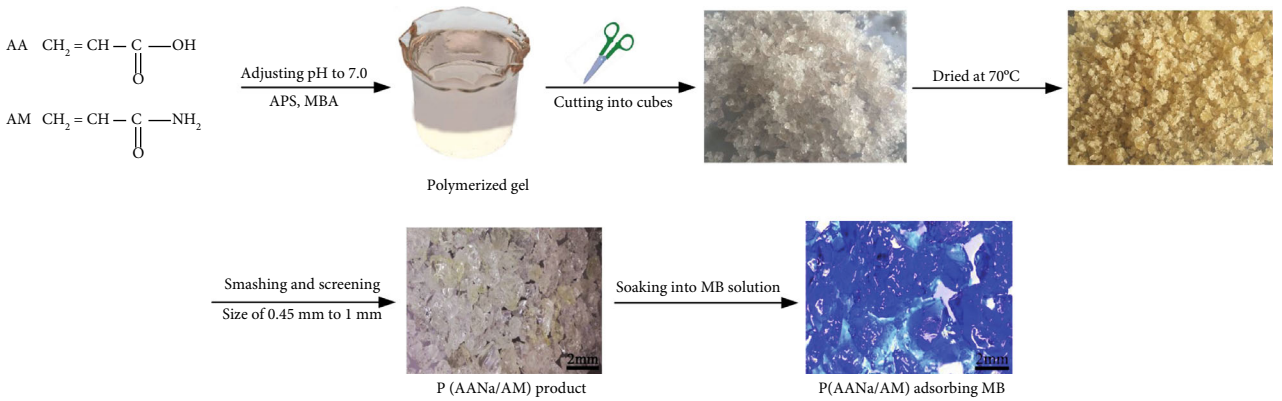

Figure 4: Morphological changes of P(AANa/AM) during the preparation and MB adsorption processes.

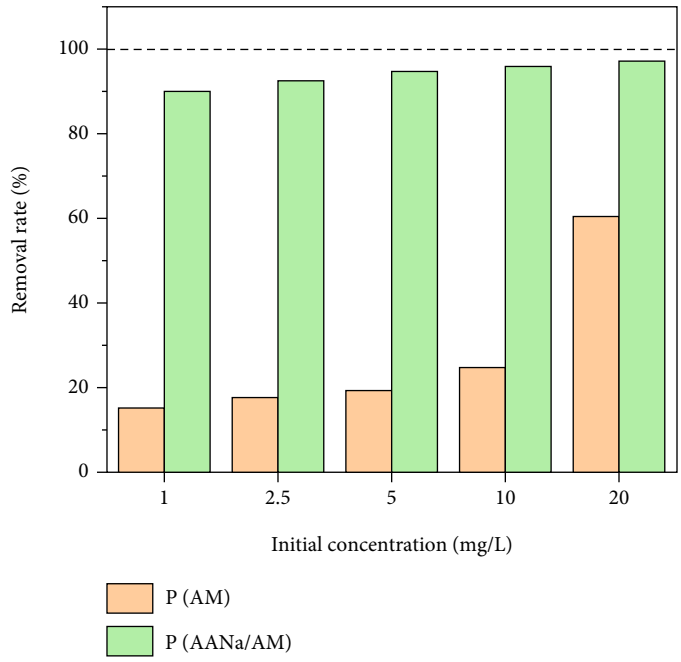

Figure 5: MB removal rates of P(AM) and P(AANa/AM).

the removal rate by P(AM) was 60.57%. However, P(AANa/AM) exhibited outstanding adsorption performance even under low MB concentration. The removal rates of P(AANa/AM) were 90.18% for 1 mg/L MB and 97.34% for 20 mg/L MB. The results demonstrated that electrostatic attraction was the most efficient adsorption mechanism. Even though -$CONH_2$ groups in P(AM) were able to bind MB molecules through hydrogen bond, a remarkable amount of MB was still presented in the solution. The removal efficiency for MB contaminants by P(AM) was subpar due to the diffusion resistance [35]. The goal of reducing a large amount of MB was not met after reaching the equilibrium condition. In comparison, P(AANa/AM) maintained an active adsorption performance with the existence of -COONa groups. According to the literature, hydrogen bond and electrostatic attraction are responsible for the adsorption functional forces [36, 37]. From these results, cationic MB molecules were concentrated on the adsorbents by anionic -COONa groups. Additionally, the -COONa groups in the stretched polymer chains might increase the negative charge of the P(AANa/AM) adsorbent by virtue of the swelling feature. After reaching equilibrium, the amount of residual dye pollutants in the solution was also minimal. By contrast, -$CONH_2$ in P(AM) exhibited dye combination property through hydrogen bond. A huge decrease in MB concentration was not obtained by P(AM). On the contrary, the excellent removal rate results by P(AANa/AM) demonstrated high efficiency in enriching the mass transfer of dye pollutants from solution into adsorbent by electrostatic attraction.

3.5. Effect of Coexisting Substance on MB Adsorption. Figure 6(a) shows the MB removal rates by P(AANa/AM) adsorbent under various coexisting Na^+ concentrations. Efficient removal results were maintained when Na^+ concentration was lower than 0.001 mol/L. Further increasing the concentration of coexisting Na^+ in MB solutions decreased the MB removal rates. The remarkable relationship between MB removal rate and coexisting Na^+ concentration indicated that high of Na^+ concentration in the solution would inhibit -COONa groups from combining with MB molecules [38, 39]. The ionization reaction of -COONa into $-COO^-$ and Na^+ occurred after P(AANa/AM) was soaked into MB solution. High concentration of Na^+ brought the ionization resistance to shield the active sites in $-COO^-$ groups. Moreover, a large amount of Na^+ in the solution caused the increase of the cationic density and produced an ion shielding effect to MB molecules [40]. Thus, the MB removal rate by P(AANa/AM) declined under 0.1 mol/L coexisting Na^+ solution. Figure 6(b) shows the MB removal rates by P(AANa/AM) under the interference of different organic compounds with the same MB concentration of 20 mg/L. The MB removal rates were 97.34%, 97.29%, and 97.04% when 20 mg/L glucose, urea, and humic acid were coexisted with 20 mg/L MB solution. Stable and excellent removal results were obtained in the interference of organic compounds. Therefore, electrostatic attraction has a potential application in adsorbents to control MB pollution.

3.6. Effect of Initial Dye Concentration on Adsorption. Figure 7 shows the MB adsorption capacity of P(AANa/AM) under various initial MB concentrations. The adsorption capacities of P(AANa/AM) increased linearly with increasing MB concentration in solution. The MB adsorption capacity of the P(AANa/AM) product was 198.29 mg/g at the initial MB concentration of 200 mg/L. Methylene blue is a water-based dye with excellent solubility. The MB removal rates at the initial MB concentration of 200 and

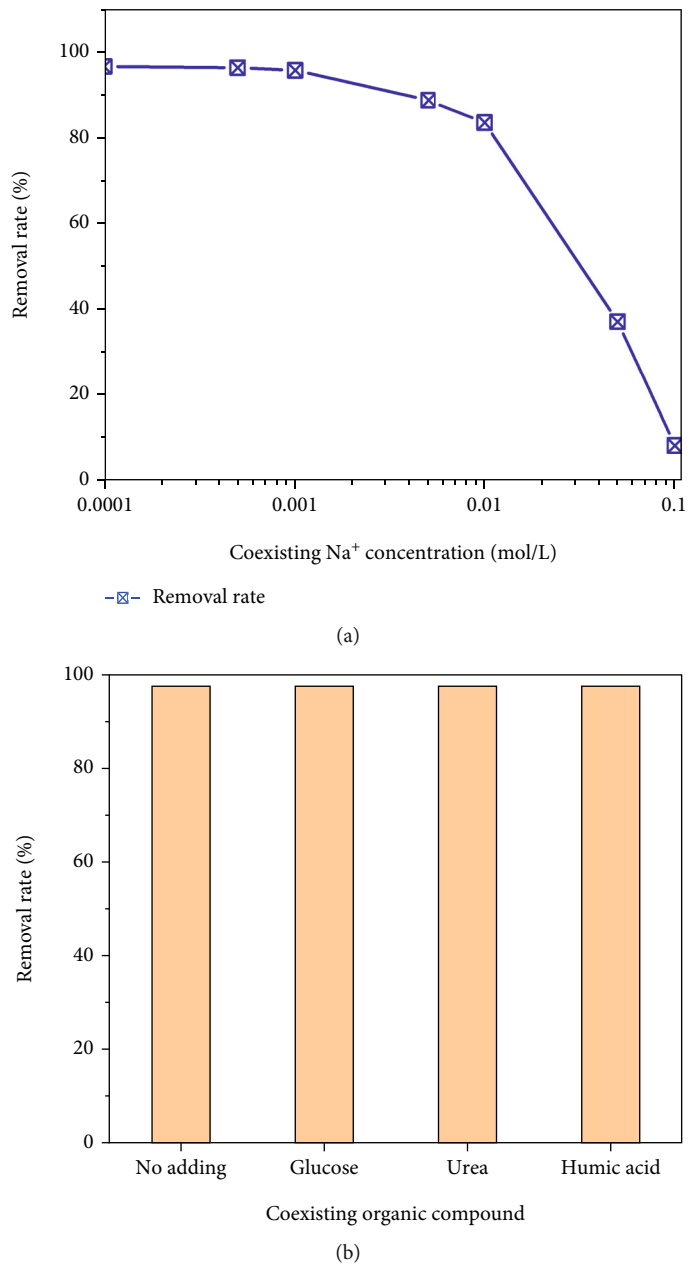

Figure 6: Effects of coexisting (a) Na^+ concentration and (b) organic compounds on MB removal rates.

1 mg/L was 98.94% and 90.18%, respectively, owing to the electrostatic attraction of -COONa to MB molecules. The experimental results indicated that electrostatic attraction has an absolute superiority in dye adsorption over other mechanisms. Different from the physical porous structure, -COONa groups enriched the mass transfer of the dye pollutant from the solution into solid adsorbents.

3.7. Column Adsorption Experiment. Figure 8 shows the apparent changes of P(AANa/AM) and MB removal rates in the column adsorption experiment. The expanding tendency of dried particles became apparent after injecting 20 mg/L MB solution. Water started trickling from the top outlet after 2 min. The MB removal rate from wastewater was 90.21% at this time. Afterward, the expansion continued as it approached water absorption saturation after 5 min. The removal rates remained consistent and effective in the following injection step. Overall, the swelling property for P(AANa/AM) was visible. An excellent interception of MB pollutants was achieved by the swollen P(AANa/AM) particles. Besides the microscopic differences in adsorbent before and after adsorbing dye pollutants, a new insight was generated that the morphological changes of adsorbents on dye adsorption should be followed.

3.8. Dye Adsorption Mechanism. Figure 9 shows the schematic illustration of the dye adsorption mechanism from individual evaluation experiments of the contributions of

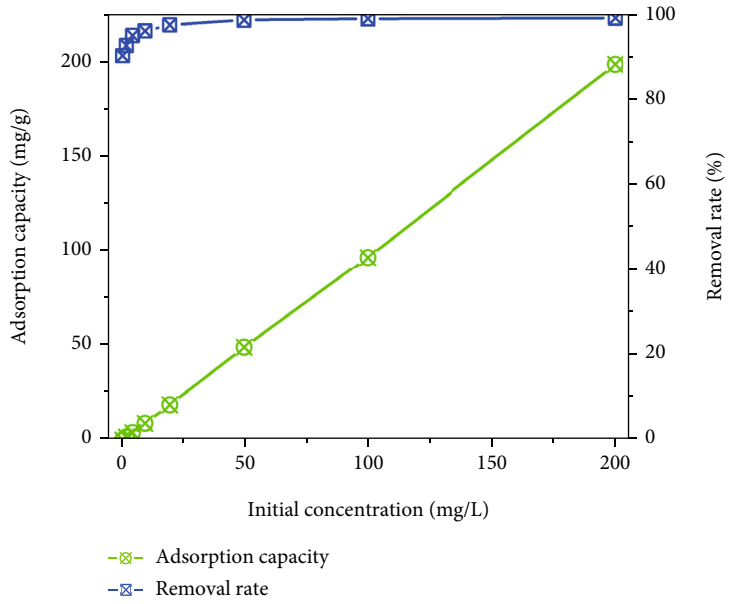

Figure 7: Effect of MB concentration on the equilibrium adsorption capacity for P(AANa/AM).

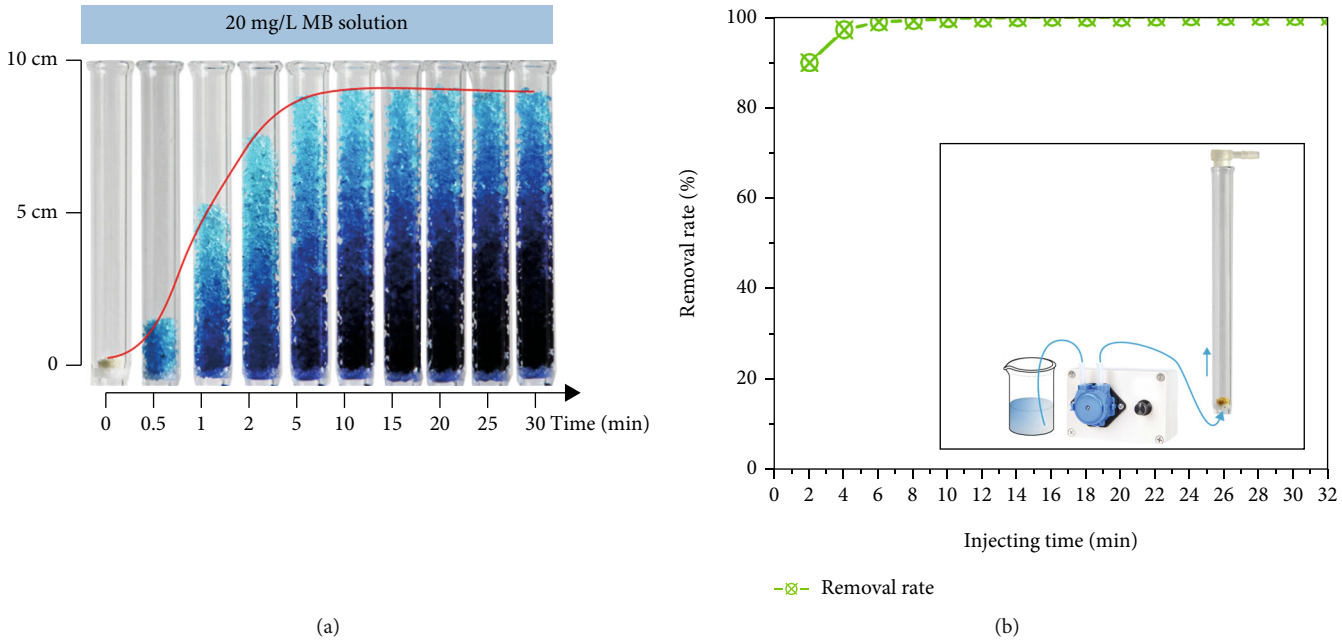

Figure 8: Dynamic changes in P(AANa/AM) morphology and MB removal rates in column adsorption experiments.

physical hole structure, hydrogen bond, and electrostatic attraction. Firstly, the physical hole structure in the material could be regarded as the space area [41]. Water molecules and its contained dye molecules could permeate into the inner area by immersing porous material in the dye solution [42]. This migration behavior was in virtue of the wetting effect. Notably, the dye concentrations in the inner area of the adsorbent and the outer solution were equal. The dye removal rate was 0% from the representative result of the porous sponge. Secondly, the existence of hydrogen bonds with N and O atoms exhibited the bonding fastness for dye pollutants. The representative results of P(AM) on dye adsorption indicated that it had low MB removal rates. The combination by hydrogen bond was limited by migration resistance, which was dominated by the dye concentration in the solution. The remarkable decrease in dye concentration was not obtained even in high P(AM) doses. The findings could confirm that the hydrogen bond between adsorbent and dye pollutants did not play a crucial role in decreasing dye concentration. Thirdly, the results by P(AANa/AM) on dye adsorption indicated that the electrostatic attraction between anionic -COONa groups and cationic MB molecules exhibited an excellent removal effect by transferring dye pollutants into adsorbents. This point

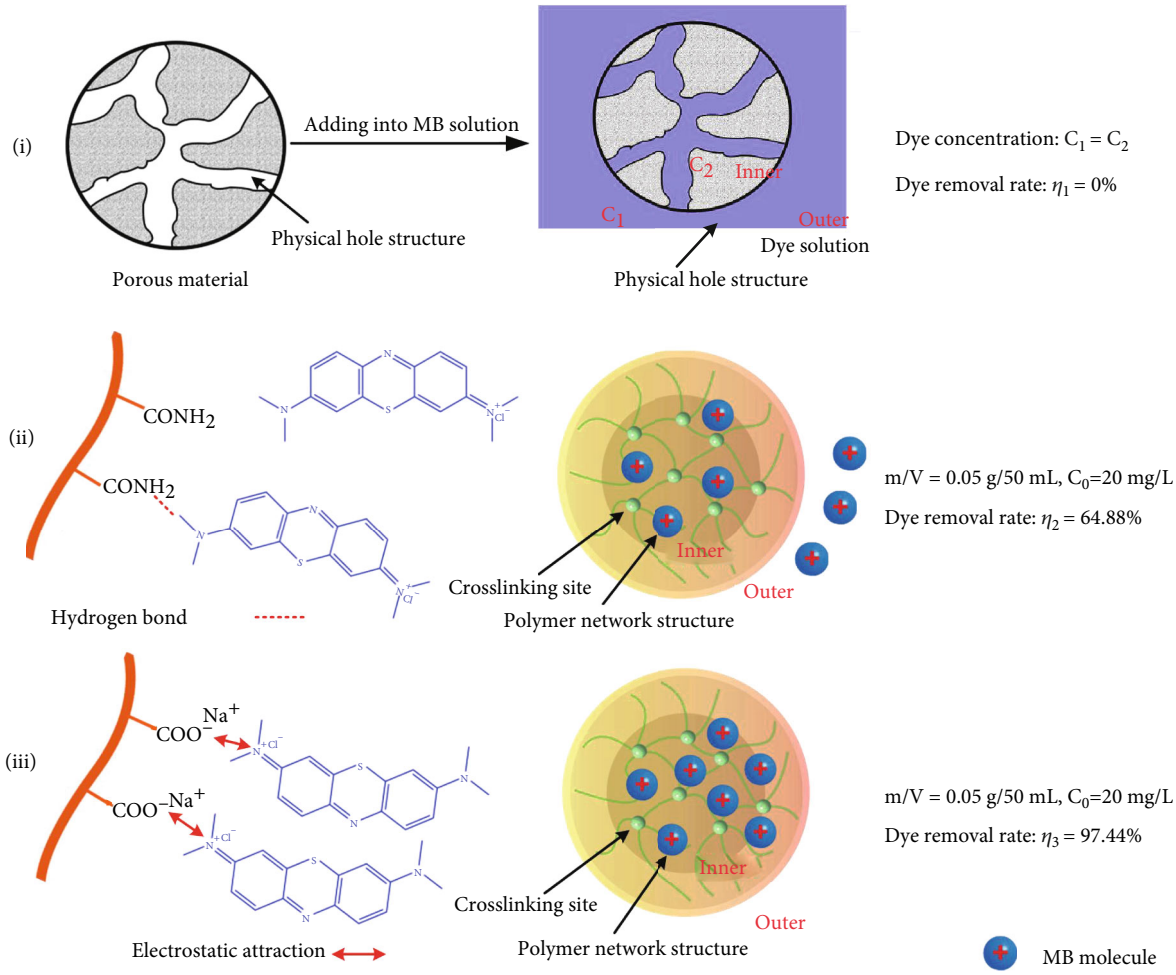

Figure 9: Schematic illustration of dye adsorption mechanism from individual evaluation experimental results.

was also supported in the shake flask and column adsorption experiments. Overall, the individual evaluation experiments defined the crucial role of electrostatic attraction in dye pollutant treatment. Moreover, an inspiration arose spontaneously that the firm statement should be validated by independent evidence, rather than just a possibility.

4. Conclusion

In summary, the contributions of physical hole structure, hydrogen bond, and electrostatic attraction to dye adsorption were studied from individual evaluation experiments. Comparisons of MB removal rates and apparent changes to sponge, P(AM), and P(AANa/AM) were conducted. The results of MB removal rates by porous sponge revealed that physical hole structure was useless in decreasing dye concentration. The low removal rate by P(AM) indicated that hydrogen bond could not substantially reduce dye concentration. The electrostatic attraction between -COONa and MB molecules achieved the enrichment of MB adsorption from solution into solid adsorbents. As one of the main synthetic materials, AM played a role in enhancing the mechanical stretch of the intermediate polymeric gel. Additionally, the findings of the morphological observation and water absorbency measurement revealed that the expanding behavior of P(AANa/AM) coexisted in MB solution. In further research, electrostatic attraction on dye adsorption should be thought highly to develop adsorbents. This study also recommends that the convincing conclusion should be obtained by visible evidence. Some individual representatives might be chosen to decompose the complex compositions of the adsorbent.

Data Availability

The data used to support the findings of this study are included within the article. Should further data or information be required, these are available from the corresponding author upon request.

Conflicts of Interest

The authors declare that there are no any conflicts of interest regarding the publication of this paper.

Supplementary Materials

To evaluate the effects of physical hole structure, hydrogen bond, and electrostatic attraction on dye adsorption, three individual perspectives were chosen. The three products that these adsorption forms matched were porous sponges with porous structure, P(AM) containing-CONH2, P(AANa/AM) containing-CONH2, and -COONa. This research might give an insight to develop and perfect dye adsorption theories. *(Supplementary Materials)*

References

[1] H. Huang, Z. Liu, J. Yun, H. Yang, and Z. L. Xu, "Preparation of Laponite hydrogel in different shapes for selective dye adsorption and filtration separation," *Applied Clay Science*, vol. 201, article 105936, 2021.

[2] V. J. Landin-Sandoval, D. I. Mendoza-Castillo, M. K. Seliem et al., "Physicochemical analysis of multilayer adsorption mechanism of anionic dyes on lignocellulosic biomasses via statistical physics and density functional theory," *Journal of Molecular Liquids*, vol. 322, article 114511, 2021.

[3] A. S. Eltaweil, G. S. Elgarhy, G. M. el-Subruiti, and A. M. Omer, "Carboxymethyl cellulose/carboxylated graphene oxide composite microbeads for efficient adsorption of cationic methylene blue dye," *International Journal of Biological Macromolecules*, vol. 154, pp. 307–318, 2020.

[4] X. Chen, C. Chen, and J. Zhu, "Facile preparation of cellulose-attapulgite nanocomposite hydrogel for dye adsorption," *Iranian Polymer Journal*, vol. 28, no. 4, pp. 347–359, 2019.

[5] Z. Chang, Y. Chen, S. Tang et al., "Construction of chitosan/polyacrylate/graphene oxide composite physical hydrogel by semi-dissolution/acidification/sol-gel transition method and its simultaneous cationic and anionic dye adsorption properties," *Carbohydrate Polymers*, vol. 229, article 115431, 2020.

[6] Z. Yang, G. Wu, C. Gan, G. Cai, J. Zhang, and H. Ji, "Effective adsorption of arsenate, dyes and eugenol from aqueous solutions by cationic supramolecular gel materials," *Colloids and Surfaces A: Physicochemical and Engineering Aspects*, vol. 616, article 126238, 2021.

[7] C. Duan, J. Wang, Q. Liu, Y. Zhou, and Y. Zhou, "Efficient removal of salbutamol and atenolol by an electronegative silanized β-cyclodextrin adsorbent," *Separation and Purification Technology*, vol. 282, article 120013, 2022.

[8] Q. Liu, Y. Li, H. Chen et al., "Superior adsorption capacity of functionalised straw adsorbent for dyes and heavy-metal ions," *Journal of Hazardous Materials*, vol. 382, article 121040, 2020.

[9] Z. W. Cui, X. L. Wang, H. Y. Lin et al., "Two Anderson-type polyoxometalate-based metal-organic complexes with a flexible bis(pyrazine)-bis(amide) ligand for rapid adsorption and selective separation of cationic dyes," *Inorganica Chimica Acta*, vol. 513, article 119937, 2020.

[10] S. Nayak, S. R. Prasad, D. Mandal, and P. Das, "Carbon dot cross-linked polyvinylpyrrolidone hybrid hydrogel for simultaneous dye adsorption, photodegradation and bacterial elimination from waste water," *Journal of Hazardous Materials*, vol. 392, article 122287, 2020.

[11] M. Mohammadikish and D. Jahanshiri, "Rapid adsorption of cationic and anionic dyes from aqueous solution via metal-based coordination polymers nanoparticles," *Solid State Sciences*, vol. 99, article 106063, 2020.

[12] P. Li, B. Gao, A. Li, and H. Yang, "Evaluation of the selective adsorption of silica-sand/anionized-starch composite for removal of dyes and Cupper(II) from their aqueous mixtures," *International Journal of Biological Macromolecules*, vol. 149, pp. 1285–1293, 2020.

[13] P. Pradhan and A. Bajpai, "Preparation and characterization of films from chicken feathers for dye adsorption," *Materials Today: Proceedings*, vol. 29, pp. 1204–1212, 2020.

[14] X. F. Tan, S. S. Zhu, R. P. Wang et al., "Role of biochar surface characteristics in the adsorption of aromatic compounds: pore structure and functional groups," *Chinese Chemical Letters*, vol. 32, no. 10, pp. 2939–2946, 2021.

[15] M. R. Razanajatovo, W. Gao, Y. Song, X. Zhao, Q. Sun, and Q. Zhang, "Selective adsorption of phosphate in water using lanthanum-based nanomaterials: a critical review," *Chinese Chemical Letters*, vol. 32, no. 9, pp. 2637–2647, 2021.

[16] T. Wang, J. He, J. Lu, Y. Zhou, Z. Wang, and Y. Zhou, "Adsorptive removal of PPCPs from aqueous solution using carbon-based composites: a review," *Chinese Chemical Letters*, vol. 33, no. 8, pp. 3585–3593, 2022.

[17] G. Wang, G. Li, Y. Huan, C. Hao, and W. Chen, "Acrylic acid functionalized graphene oxide: high-efficient removal of cationic dyes from wastewater and exploration on adsorption mechanism," *Chemosphere*, vol. 261, article 127736, 2020.

[18] P. M. Morais da Silva, N. G. Camparotto, T. Figueiredo Neves et al., "Effective removal of basic dye onto sustainable chitosan beads: batch and fixed-bed column adsorption, beads stability and mechanism," *Sustainable Chemistry and Pharmacy*, vol. 18, article 100348, 2020.

[19] M. Chen, Y. Shen, L. Xu, G. Xiang, and Z. Ni, "Highly efficient and rapid adsorption of methylene blue dye onto vinyl hybrid silica nano-cross-linked nanocomposite hydrogel," *Colloids and Surfaces A: Physicochemical and Engineering Aspects*, vol. 613, article 126050, 2021.

[20] M. Y. Xu, H. L. Jiang, Z. W. Xie, Z. T. Li, D. Xu, and F. A. He, "Highly efficient selective adsorption of anionic dyes by modified β-cyclodextrin polymers," *Journal of the Taiwan Institute of Chemical Engineers*, vol. 108, pp. 114–128, 2020.

[21] J. Fan, Z. Shi, M. Lian, H. Li, and J. Yin, "Mechanically strong graphene oxide/sodium alginate/polyacrylamide nanocomposite hydrogel with improved dye adsorption capacity," *Journal of Materials Chemistry A*, vol. 1, no. 25, p. 7433, 2013.

[22] S. D. K. Seera, D. Kundu, P. Gami, P. K. Naik, and T. Banerjee, "Synthesis and characterization of xylan-gelatin cross-linked reusable hydrogel for the adsorption of methylene blue," *Carbohydrate Polymers*, vol. 256, pp. 117520–117520, 2021.

[23] H. Hafdi, M. Joudi, J. Mouldar et al., "Design of a new low cost natural phosphate doped by nickel oxide nanoparticles for capacitive adsorption of reactive red 141 azo dye," *Environmental Research*, vol. 184, article 109322, 2020.

[24] H. L. Jiang, M. Y. Xu, Z. W. Xie, W. Hai, X. L. Xie, and F. A. He, "Selective adsorption of anionic dyes from aqueous solution by a novel β-cyclodextrin-based polymer," *Journal of Molecular Structure*, vol. 1203, article 127373, 2020.

[25] D. Tang, Z. Xiong, P. Lu et al., "Lacunary polyoxometalate @ ZIF for ultradeep Pb(II) adsorption," *Chemical Engineering Science*, vol. 262, article 118003, 2022.

[26] J. Zhu, X. Lou, Y. Wang, Z. Xiong, J. Chen, and W. Yan, "Conjugated microporous poly(aniline)s for removal of low-concentration formaldehyde," *Chemical Engineering Science*, vol. 248, article 117119, 2022.

[27] G. B. Marandi, M. Baharloui, M. Kurdtabar, L. M. Sharabian, and M. A. Mojarrad, "Hydrogel with high laponite content as nanoclay: swelling and cationic dye adsorption properties," *Research on Chemical Intermediates*, vol. 41, no. 10, pp. 7043–7058, 2015.

[28] D. Li, Q. Li, N. Bai, H. Dong, and D. Mao, "One-step synthesis of cationic hydrogel for efficient dye adsorption and its second use for emulsified oil separation," *ACS Sustainable Chemistry & Engineering*, vol. 5, no. 6, pp. 5598–5607, 2017.

[29] S. Karakuş, N. Taşaltın, C. Taşaltın, and A. Kilislioğlu, "Comparative study on ultrasonic assisted adsorption of Basic Blue 3, Basic Yellow 28 and Acid Red 336 dyes onto hydromagnesite stromatolite: kinetic, isotherm and error analysis," *Surfaces and Interfaces*, vol. 20, article 100528, 2020.

[30] T. Vidhyadevi, M. Arukkani, K. Selvaraj, P. M. Periyaraman, R. Lingam, and S. Subramanian, "A study on the removal of heavy metals and anionic dyes from aqueous solution by amorphous polyamide resin containing chlorobenzalimine and thioamide as chelating groups," *Korean Journal of Chemical Engineering*, vol. 32, no. 4, pp. 650–660, 2015.

[31] M. Pasichnyk, M. Václavíková, and I. Melnyk, "Fabrication of polystyrene-acrylic/ZnO nanocomposite films for effective removal of methylene blue dye from water," *Journal of Polymer Research*, vol. 28, no. 2, p. 56, 2021.

[32] B. Eftekhari-Sis, V. Rahimkhoei, A. Akbari, and H. Y. Araghi, "Cubic polyhedral oligomeric silsesquioxane nano-cross-linked hybrid hydrogels: synthesis, characterization, swelling and dye adsorption properties," *Reactive and Functional Polymers*, vol. 128, pp. 47–57, 2018.

[33] X. Lou, J. Chen, Z. Xiong et al., "Porosity design on conjugated microporous poly(aniline)s for exceptional mercury(II) removal," *ACS Applied Materials & Interfaces*, vol. 13, no. 51, pp. 61653–61660, 2021.

[34] J. Chen, R. Dong, S. Chen et al., "Selective adsorption towards heavy metal ions on the green synthesized polythiophene/MnO_2 with a synergetic effect," *Journal of Cleaner Production*, vol. 338, article 130526, p. 130536, 2022.

[35] W. Kangwansupamonkon, N. Klaikaew, and S. Kiatkamjornwong, "Green synthesis of titanium dioxide/acrylamide-based hydrogel composite, self degradation and environmental applications," *European Polymer Journal*, vol. 107, pp. 118–131, 2018.

[36] Y. Chen, L. Li, Y. Li et al., "Preparation of a double-network hydrogel based on wastepaper and its application in the treatment of wastewater containing copper(II) and methylene blue," *RSC Advances*, vol. 11, no. 29, pp. 18131–18143, 2021.

[37] H. M. Abdel-Aziz and T. Siyam, "Radiation synthesis of poly(-acrylamide-acrylic acid-dimethylaminoethyl methacrylate) resin and its use for binding of some anionic dyes," *Water, Air, and Soil Pollution*, vol. 218, no. 1-4, pp. 165–174, 2011.

[38] D. Kaner, A. Saraç, and B. F. Şenkal, "Removal of dyes from water using crosslinked aminomethane sulfonic acid based resin," *Environmental Geochemistry and Health*, vol. 32, no. 4, pp. 321–325, 2010.

[39] Y. Tang, X. Wang, and L. Zhu, "Removal of methyl orange from aqueous solutions with poly(acrylic acid-co-acrylamide) superabsorbent resin," *Polymer Bulletin*, vol. 70, no. 3, pp. 905–918, 2013.

[40] S. Emik, S. Işık, and E. Yıldırım, "Simultaneous removal of cationic and anionic dyes from binary solutions using carboxymethyl chitosan based IPN type resin," *Journal of Polymers and the Environment*, vol. 29, no. 6, pp. 1963–1977, 2021.

[41] X. Lou, X. Chen, D. Tang et al., "Conjugated microporous poly(aniline) enabled hierarchical porous carbons for Hg(II) adsorption," *Langmuir*, vol. 38, no. 43, pp. 13238–13247, 2022.

[42] A. A. Adeyi, S. N. A. M. Jamil, L. C. Abdullah, T. S. Y. Choong, K. L. Lau, and M. Abdullah, "Adsorptive removal of methylene blue from aquatic environments using thiourea-modified poly(acrylonitrile-co-acrylic acid)," *Materials*, vol. 12, no. 11, p. 1734, 2019.